Hybrid CFD/FEM calculations for the aero-acoustic noise radiated from a radial fan

Hakan Dogan
Department of Mathematics, Physics and Chemistry, Beuth University of Applied Sciences, Berlin, Germany.

Chris Eisenmenger
School of Engineering – Technology and Life, HTW University of Applied Sciences, Berlin, Germany.

Martin Ochmann
Department of Mathematics, Physics and Chemistry, Beuth University of Applied Sciences, Berlin, Germany.

Stefan Frank
School of Engineering – Technology and Life, HTW University of Applied Sciences, Berlin, Germany.

Summary
In this work, hybrid numerical simulations for the aeroacoustic noise of a radial fan are presented. The geometry of the problem is set up according to an experimental technique: the so-called "In-Duct" method described by the industrial norm DIN EN ISO 5136. Three slit-tube microphones inside a circular duct are used to monitor the far-field noise levels. The operating radial fan has a diameter of 200 mm and is of backward-curved type with nine blades. The direct fluid dynamics simulations for the whole system are computationally expensive. Hence, a hybrid approach is employed for the aeroacoustic noise. The near field pressure and velocity values are computed with CFD (using ANSYS software), and the far field acoustic pressure is evaluated performing a coupling of the numerical code with the finite element software COMSOL. In particular, the Stress Blended Eddy Simulation (SBES) is employed in CFD computations. A virtual interface near the beginning section of the duct is used for the data exchange. The acoustic pressure at the locations of probe microphones in the far-field is computed using the FEM. Sound pressure levels inside the duct predicted by these numerical methods are presented and comparison of the numerical results with the experimental values is also shown.

PACS no. 43.28.Ra

1. Introduction

The axial and the radial fans are used in many commercial applications such as the heating/cooling systems in automobiles and home appliances [1]. The major concerns when improving the design of such fans are to increase the aerodynamic efficiency and to decrease the aeroacoustic noise. Some brief methods regarding the aerodynamic performance are adjusting the number of blades and their structure, i.e. using backward, forward or mixed type skewed blades [2]. The aeroacoustic noise, on the other hand, is strongly dependent on the aerodynamics, owing to the unsteady pressure fluctuations on the fan blades and the shear stresses. These effects create a broadband noise and a high amplitude tonal component at the blade passing frequency [3].

In the present article, experimental and numerical investigations of the aerodynamic and aeroacoustic characteristics of a radial fan with backward curved blades are performed. For the numerical calculations, since the CFD simulations for the whole system would be computationally expensive, we employ a hybrid CFD – computational aeroacoustics (CAA) approach here. The geometry of the problem is given in Fig. 1a, where the center

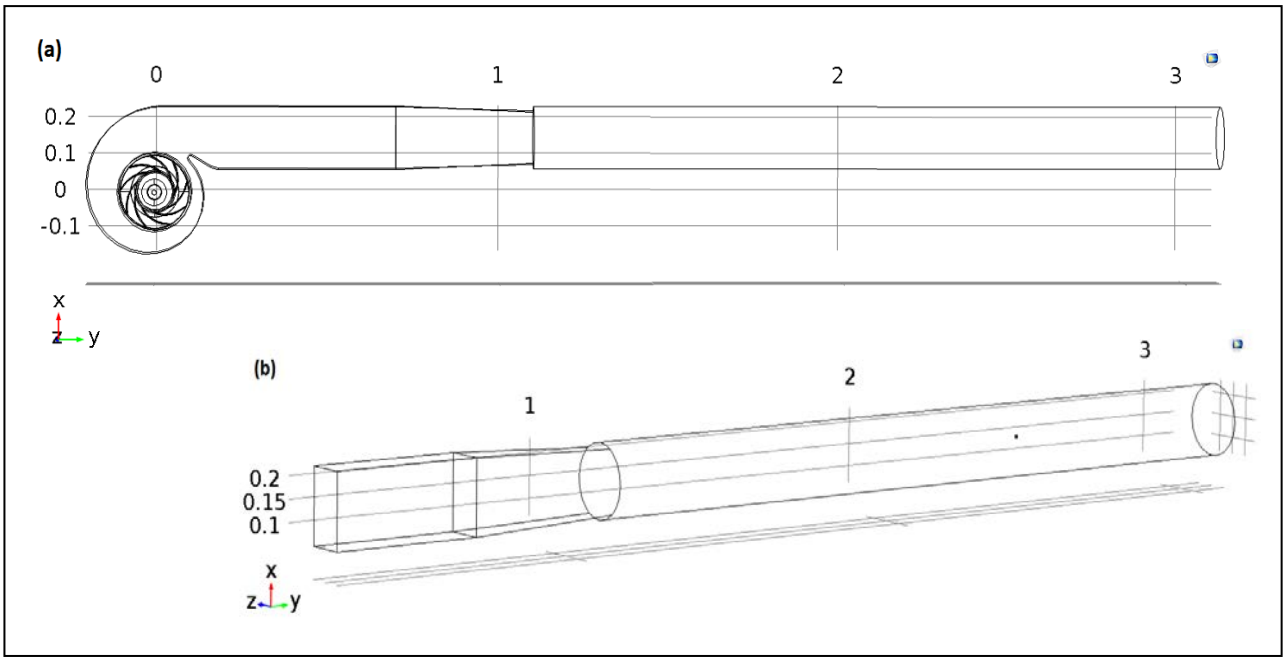

Figure 1. The problem geometry: (a) the complete experimental setup shown in the *x*-*y* plane and (b) the isometric view of the acoustic computation domain.

of the rotor is located at y=0, the airflow is provided into the fan in –z direction, and the region y<0.7m constitutes the domain for the CFD computations, i.e. the near field. The CFD computations are performed in this region using ANSYS-CFX [4]. The section of the duct where $0.7 < y < 1.1$ is the transition part; the cross-section of the duct changes from rectangular to circular. The remaining part of the geometry (y > 1.1m) is the circular duct.

In order to implement a hybrid aeroacoustic simulation, a virtual interface is located after the volute (step) tongue of the fan. This location is particularly chosen because the velocity field reaches a quasi-uniform behavior in the discharge duct. Therefore, the acoustic computation domain is defined as in Fig. 1b. The numerical computations to evaluate the sound pressure levels in the far field has been performed using the frequency domain pressure acoustics module in COMSOL [5].

In terms of aeroacoustic modeling, several approaches and formulations may be found in the literature. In Ref. [6], the well-known Ffowcs Williams – Hawkings equation was used together with analytical formulas for the monopole and dipole sources acting on the blades of a centrifugal fan. In Ref. [7], a surface integral method was applied to interior duct acoustics for the noise predictions of a backward curved radial fan, whereas Ref. [8] studies the aeroacoustic characteristics of an axial fan using the perturbed convective acoustic equations. In Ref. [9], boundary element method and equivalent source method were implemented to compute the thermo-aeroacoustic noise caused by flames. Oberai et al. [10] have presented a frequency domain form of Lighthill's inhomogeneous wave equation accounting for the effects of the mean flow. Moreover, they have proposed the concept of a permeable surface between the CFD (near field) and acoustic (far) field, and applied such approach to an exterior propagation problem over an airfoil. In the present paper, we use the same method based on the permeable (virtual) interface, and apply it to interior (duct) acoustics.

2. Experimental setup

Two different experimental test facilities were used in order to demonstrate the characteristic curves and the performance of the designed fan. The first one is a chamber test rig built in accordance with ISO 5801 [11], where the volumetric flow rate is varied over a constant rotational speed and the pressure rise and the torque acting on the fan is measured. This test is done to evaluate the optimal performance of the fan and the best efficiency point.

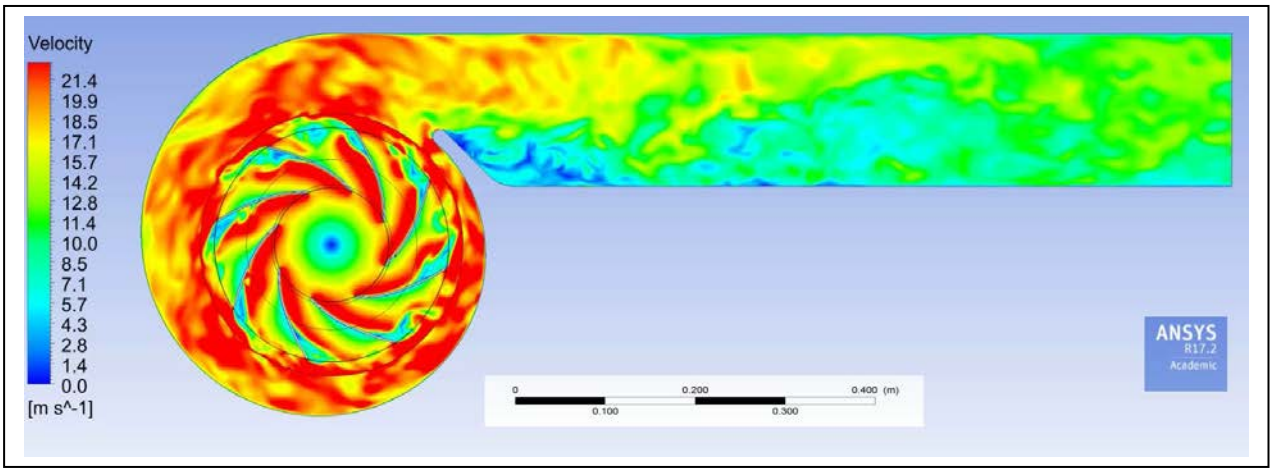

Figure 2. The magnitude of the velocity vector obtained from CFD simulations using ANSYS.

The acoustic noise measurements were carried out according to the international norm ISO 5136 [12] using the in-duct method. The test facility (in Fig. 1a) was installed inside a semi-anechoic room. Although not shown in the figure, an anechoic termination was mounted to the outlet (at y=3.1 m). Three high precision slit-tube microphones were installed inside the duct on x-z plane, at y=2.47m.

The noise recordings were done with a duration of 35 seconds and were repeated ten times in order to reduce the standard deviation error of the results. The Fourier transform of the time signals were computed with the software Samurai from Sinus Acoustics, and the obtained sound pressure levels (SPLs) were averaged over ten samples. The final displayed results for the noise levels require some corrections because of the mean flow velocity and the shield protection of the slit microphones. The details of such adjustments can be found in [12].

3. Computational Fluid Dynamics

The computational fluid dynamics simulations have been performed within the near field as defined above. Stress Blended Eddy Simulations (SBES) based on the Shear Stress Transport (SST) turbulence model have been performed. The computation domain is split into three parts, where the flow field in the volume containing the fan blades is computed in a rotating frame, and the inlet and the discharge duct are set as stationary.

Full matching boundary conditions between the stationary and the rotating domains were applied as in Ref. [13].

The mesh consisted of approximately 30 million nodes with mainly tetrahedral elements, where 12-15 prism layers were created on every solid wall, including the blades, to resolve the boundary layers.

The volumetric flow and the rotational speed of the simulation were set as $\dot{V}$=450 m^3/h and n=2860 rpm, respectively. The time step was chosen as equivalent to 1° rotation of the fan, which is equal to Δt= 5.828 × 10^{-5} s. For the given parameters, the static efficiency of the fan is calculated using

$$\eta_{\mathrm{st}} = \frac{\dot{V}\,\Delta p}{M_{\mathrm{T}} 2\pi n}, \qquad (1)$$

where Δp is the pressure difference between the inlet and the outlet, and M_{T} is the total torque acting on the whole rotor.

In Fig. 2, the results of the CFD simulation are shown at a certain time instant, where the magnitude of the velocity vector is plotted in the x-y plane. It can be observed that approximately 0.2m after the volute tongue, towards the outlet of the fan, the velocity vector exhibits a near-uniform behaviour, i.e. a mean flow with Mach number M<0.03 can be assumed in this region.

The Lighthill stress tensor is related to the autocorrelation and cross-correlations of the velocity components. When such components are important noise sources, the solution of the inhomogeneous wave equation is required, as explained in Sec 4. In the exhaust duct, the component in the direction of the flow is expected to be the dominant one over the others. In Fig. 3, T_{yy} component of the Lighthill tensor, as obtained from the CFD simulation, is shown.

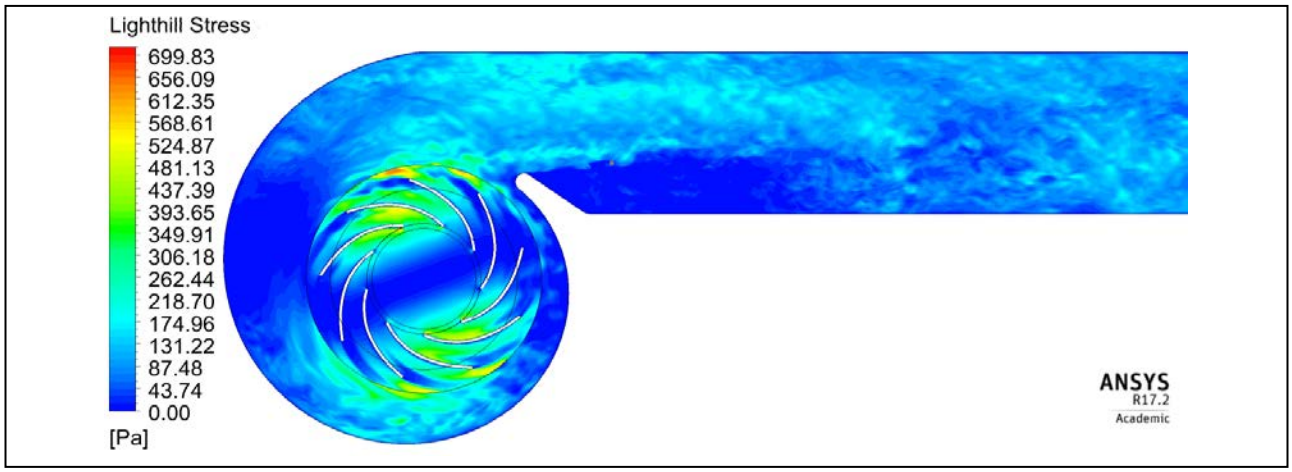

Figure 3. The T_{yy} component of the Lighthill stress tensor from CFD simulations.

4. Acoustic computations

The frequency domain acoustic wave equation accounting for the turbulent shear stresses is given by [10]

$$\nabla^2 p + k^2 p = \frac{\partial \tilde{T}_{ij}}{\partial x_i \partial x_j}, \qquad (2)$$

where $\tilde{T}_{ij}$ is Fourier transform of the Lighthill stress tensor T_{ij}, and p is the acoustic pressure. The boundaries of the acoustic computation domain are as follows: The permeable surface created at the rectangular cross-section of the duct is denoted as Γ_{I}, the rigid walls between the permeable interface and the duct outlet is denoted as Γ_{w}, and the outlet surface is denoted as Γ_{o}.

In order to investigate the effect of the location of the permeable interface on the SPL, we perform simulations with three different arrangements, namely locating the interface at three positions: y=0.2m, y=0.3m, and y=0.4m. Accordingly, the total length of the acoustic computation domain is different for the three cases, as well as the length of the boundary defined as rigid walls (Γ_{w}). Though, note that the positions of the microphones are fixed in the numerical calculations, as well as in the experimental setup. As such, for the acoustic computations, in all three cases, we prescribe the full reflection condition on the rigid walls, i.e.

$$\frac{\partial p(\boldsymbol{x})}{\partial n} = 0 \qquad \boldsymbol{x} \in \Gamma_{\mathrm{w}}. \qquad (3)$$

At the outlet, the impedance boundary condition is employed in order to ensure no-reflection of the acoustic waves, i.e.

$$Z(\boldsymbol{x}) = 1.2 \times 343 \ [\mathrm{kg/m^2 s}], \qquad \boldsymbol{x} \in \Gamma_{\mathrm{o}}. \qquad (4)$$

At the permeable interface, the pressure is prescribed as the boundary condition. As we solve for the frequency domain acoustics, the pressure on this surface is obtained using the Fourier transform, i.e.

$$p(\boldsymbol{x}, \omega) = \int_{-\infty}^{\infty} p_t(\boldsymbol{x})\, e^{-i\omega t}\, dt, \qquad \boldsymbol{x} \in \Gamma_{\mathrm{I}}, \qquad (5)$$

where p_t is the time domain variation of the hydrodynamic pressure calculated in the CFD simulations at the interface Γ_{I}. The time domain CFD results have been exported for four revolutions of the fan for each of the three simulations and the calculated far field noise levels at the microphone locations are presented in the following subsections.

4.1. Results for y=0.2 m plane

First, we present the results for the permeable interface which is nearest to the volute tongue. In Fig. 4, the sound pressure results obtained from the numerical simulation are compared with the measured experimental values.

The experimental data at the blade passing frequency (BPF) of the fan indicates a SPL of 85dB. The numerical result at this frequency only differs by 1dB compared to the experimental data.

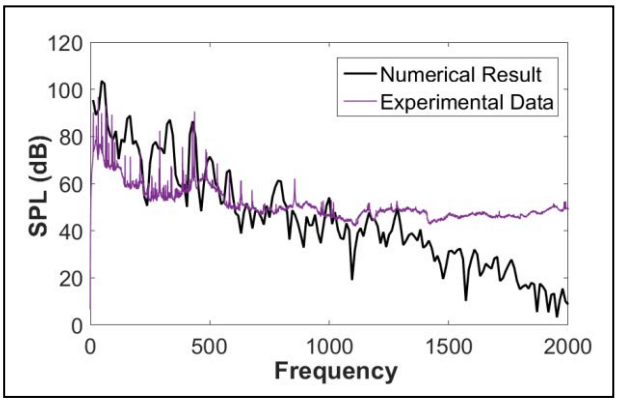

Figure 4. The SPL at the position of the microphones obtained using the permeable interface at y=0.2m

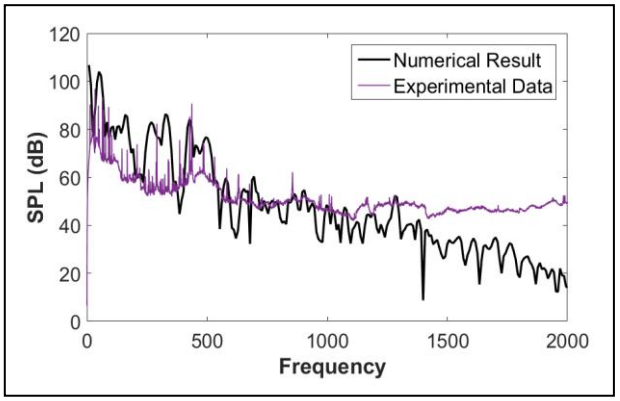

Figure 5. The SPL at the position of the microphones obtained using the permeable interface at y=0.3m

Moreover, a good agreement between the numerical and the experimental results is observed at the frequency range 500-1000 Hz. The results deviate substantially above the cut-off frequency of the duct, e.g. above 1150 Hz.

4.2. Results for y=0.3 m plane

In Fig. 5, the results obtained using the permeable interface located at y=0.3m are shown, and compared with the experimental results. The SPL calculated at the BPF is ~86 dB; therefore, it only differs by less than 1 dB in comparison to the experimental data.

Similar to the results in Sec. 4.1, a good agreement in comparison to the experimental data is observed within the mid-frequency range (500-1000 Hz).

In the low frequency range, the numerical results show two unexpected discrete peaks at around 165 Hz and 330 Hz, and substantially higher sound pressure levels are calculated compared to the experimental data. The reasons for these discrepancies are unknown to the authors. However, further CFD simulations will be performed using a shorter time step, which may provide more accurate predictions for the unsteady fluctuations of the field variables. Moreover, the frequency resolution of the current simulations is $\Delta f \approx 8$ Hz. Using a shorter time step in the time domain simulations also improves the frequency resolution in the acoustic calculations, which may lead to more accurate numerical results in the whole frequency range.

4.3. Results for y=0.4 m plane

Finally, the results obtained using the permeable interface positioned at y=0.4m are shown in Fig. 6. The sound pressure level calculated at the BPF using this interface is approximately 93 dB, which is ~8 dB higher than the experimental data and the numerical results in Figs. 4 and 5.

The low frequency region results (in the range below the BPF), and the above cut-off frequency results obtained using the y=0.4m interface show similar behavior with results obtained using the y=0.2m and the y=0.3m interface.

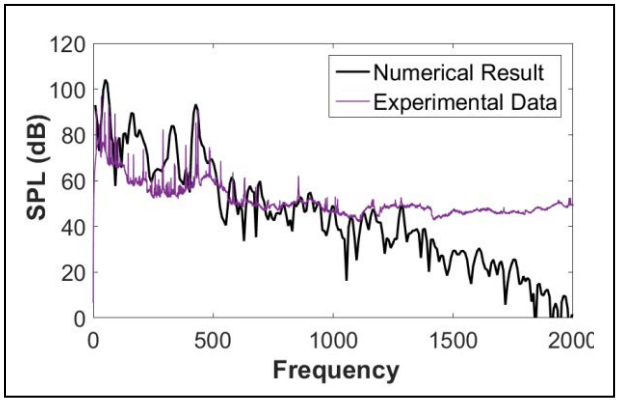

Figure 6. The SPL at the position of the microphones obtained using the permeable interface at y=0.4m.

5. Conclusions

In this work, hybrid numerical simulations to predict the aeroacoustic noise radiated from a backward curved radial fan have been performed. The CFD simulations were done in the near field where unsteady/turbulent flow structure is

substantially pronounced. The accuracy of the near field CFD simulations was verified against the theoretical estimations for the static efficiency of the fan. The permeable interface approach has been used to transfer the data to the acoustic domain, and then to compute the sound pressure level in the far field. The results have been compared to the experimental data acquired using the in-duct measurement technique as described in the international standard ISO 5136.

Overall, the hybrid CFD/FEM simulations have shown that accurate predictions of the sound pressure levels, especially at the blade passing frequency, can be achieved. The location of the data exchange interface has been tested using three different positions, and has shown to have minor effects on the predicted noise levels. However, the numerical results will be further refined by several improvements such as using a finer time step in the CFD.

The current results do not include the right hand side terms in Eq. (2) originating from the turbulent shear stresses. Further work will focus on including such domain terms in the FEM calculations.

The convective effects for the Mach number values encountered in the longitudinal duct are negligible within the acoustic domain employed here. However, these effects might be more pronounced near the fan blades. In Ref. [14], a numerical method for the convective acoustic propagation with higher Mach numbers was presented, which can be employed to the current problem as a future task.

Acknowledgement

The authors wish to thank the BMBF and the project partners ANSYS, B/S/H and GRONBACH for their support.

GEFÖRDERT VOM
Bundesministerium für Bildung und Forschung

FORSCHUNG AN FACHHOCHSCHULEN

References

[1] M. Darvish, S. Frank, C. O. Paschereit: Numerical and experimental study on the tonal noise generation of a radial fan. Journal of Turbomachinery 137 (101005) (2015) 1-9.

[2] F. Zenger, J. Müller, S. Becker: Investigation of aeroacousitc properties of low-pressure axial fans with different blade stacking. Proc. AIAA/CEAS 2017, 3389 (1-15).

[3] J. Zhang, W. Chu, H. Zhang, Y. Wu, W. Dong: Numerical and experimental investigations of the unsteady aerodynamics and aero-acoustic characteristics of a backward curved blade centrifugal fan. Applied Acoustics 110 (2016) 256-267.

[4] ANSYS-CFX, URL: http://www.ansys.com/Products/Fluids/ANSYS-CFX

[5] COMSOL Multiphysics, URL: https://www.comsol.com/acoustics-module

[6] S. Khelladi, S. Kouidri, F. Bakir, R. Rey: Predicting tonal noise from a high rotational speed centrifugal fan. Journal of Sound and Vibration 313 (2008) 113-133.

[7] N. Papaxanthos, E. Perrey-Debain, S. Bennouna, B. Ouedraogo, S. Moreau, J. M. Ville: Pressure-based integral formulations of Lighthill-Curle's analogy for internal aeroacoustics at low Mach numbers. Journal of Sound and Vibration 393 (2017) 176-186.

[8] M. Kaltenbacher, A. Hüppe, A. Reppenhagen, F. Zenger, S. Becker: Computational aeroacoustics for rotating systems with application to an axial fan. AIAA Journal 55(11) (2017) 3831-3838.

[9] R. Piscoya, H. Brick, M. Ochmann, P. Költzsch: Equivalent source method and boundary element method for calculating combustion noise. Acta Acustica United with Acustica 94 (2008) 514-527.

[10] A.A. Oberai, F. Roknaldin, T. J. R. Hughes: Computational procedures for determining structural-acoustic response due to hydrodynamic sources. Computer Methods in Applied Mechanics and Engineering 190 (2000) 345-361.

[11] Industrial Organization for Standardization, ISO 5801: Industrial Fans – Performance testing using standardized airways (2011) London.

[12] Industrial Organization for Standardization, ISO 5136: Acoustics – Determination of sound power radiated into a duct by fans and other air-moving devices (2003) London.

[13] C. Eisenmenger, S. Frank, H. Dogan, M. Ochmann: High Efficiency Low Noise Heatpump Dryer (HELNoise). Proc. 43. Jahrestagung für Akustik-DAGA (2017) 1491-1494.

[14] H. Dogan, C. Eisenmenger, M. Ochmann, S. Frank: A LBIE-RBF solution to the convected wave equation for flow acoustics. Engineering Analysis with Boundary Elements (2018) In Press, DOI: doi.org/10.1016/j.enganabound.2017.11.016